# WINTER WARMING INDICATED BY RECENT TEMPERATURE AND PRECIPITATION ANOMALIES[1]

Wendell Tangborn
*Hymet, Inc., 19001 Vashon Highway SW, Suite 201, Vashon, Washington 98070*

*Abstract*: Analysis of daily maximum and minimum temperatures and precipitation observations for the 1932–1999 period at 74 weather stations in the United States, Europe, Asia, and Australia suggests that an abrupt climate change occurred in the 1980s. Five variables are considered, namely the daily maximum, minimum, and mean temperatures, precipitation, and the diurnal temperature range. Daily departures (anomalies) of five observed variables relative to an early base period (1932–1950) are calculated for each station for the test period (1951–1999), and a 74-station daily average made for each variable. Based on these global[2] averages, five main results are presented: (1) Since 1985, there is a significant increase in positive anomalies of winter temperatures during the season approximately defined by the Northern Hemisphere winter solstice and spring equinox; positive anomalies range from 2° to 8°C for individual Northern Hemisphere stations. Seasonal warming during the Northern Hemisphere winter also occurs in the Southern Hemisphere, but to a lesser degree. (2) Beginning about 1990, positive temperature anomalies at nearly all stations are synchronized (having positive anomalies on the same day) during the winter-warming season. There is an inexplicable similarity in the seasonal patterns of temperature departures and the fraction of synchronized stations. (3) Temperature and precipitation anomalies since at least 1951 have been increasing at approximately the same rate during the winter season. The positive precipitation anomalies since the mid-1990s are strongly correlated ($r = 0.9$) with the minimum temperature anomalies. (4) Both precipitation anomalies during the Northern Hemisphere winter season and mean temperature anomalies during the Southern Hemisphere summer season are bimodal and appear to be physically linked. (5) When the mean daily temperature anomalies are segregated into separate categories using the diurnal temperature range and precipitation anomalies, there is an abrupt and consistent rise in cumulative positive temperature anomalies after 1985, suggesting a positive feedback fueled by atmospheric water vapor. The impact of warmer winters include effects on hydroelectric generation, energy consumption, water supplies, glaciers, agriculture, ocean salinity, fisheries, and ski resorts.

## INTRODUCTION

Recent studies suggest that for the past two decades the Earth's wintertime surface temperatures have increased more rapidly than during the remainder of the year. Several possible causes have been proposed. Winter warming in Europe during the 1948–1995 period appears to be linked to warm maritime air brought into Europe by

[1]Thanks to Lowell A. Rasmussen for a comprehensive and valuable review, to Reggie Muskett for the map, and to Andrew Tangborn for advice and encouragement. Funding was provided by HyMet Inc.

[2]"Global," as it is used in this study, refers to weather data collected at 74 weather stations in the United States, Europe, Asia, and Australia.



*Polar Geography*, 2003, **27**, No. 4, pp. 320-338.

winds originating in the southwestern North Atlantic (Otterman et al., 2002). However, from 1996 to 2001 this trend appears to have been interrupted. Temperatures in 1995–1996 were especially low in Europe, and moderately low over much of the Earth. Northern Hemisphere winter warming during the 1977–1994 period is associated with atmospheric circulation anomalies (Wallace et al., 1996; Zhang et al., 1997). Significant cold-season warming was observed during the 1977–1994 period, relative to the 1946–1976 reference period. Temperature and pressure anomalies during the latter period were found to have two components, one in response to sea-surface temperature (SST) anomalies, the other associated with lower-level ozone depletion (Volodin and Galin, 1999).

Polar winds play an important role in the wintertime climate of the Northern Hemisphere (Shindell et al., 2001). For the past half-century, changes in precipitation, an index of atmospheric water vapor, are believed to be caused by global warming, and may also affect global warming because they provide a positive feedback (Dai et al., 1997a, 1997b). Higher surface temperatures produce greater evaporation from the oceans and warmer air holds more moisture; both translate to increased concentrations of atmospheric water vapor, a potent greenhouse gas, which causes even higher temperatures. Higher concentrations of water vapor also produce higher rates of precipitation. Precipitation in the Northern Hemisphere has systematically increased over the past 100 years (ibid.). The link between temperature changes and precipitation (or water vapor and cloud cover) defines a positive feedback mechanism that is suggested to be a probable cause of increasing surface temperatures (Wetherald and Manabe, 1980). Analyses of cloud cover and water vapor observations in the tropics suggest a negative feedback effect, so that increasing temperatures tend to reduce upper-level clouds and increase outgoing longwave radiation (Lindzen et al., 2001). However, model simulations of doubled $CO_2$ atmospheric concentrations indicate surface warming of 5.1°C, partly due to an increase in upper-level cloud cover, a positive greenhouse effect (Rind et al., 1998). A comparison of simulated temperatures and greenhouse gases shows a high positive correlation in the Northern Hemisphere except in the summer, when the greenhouse signal is weakest (Russell et al., 2000). Based on an earlier study, there were two periods of warming during the 20th century, from 1925–1944 and 1978–1997, in which the December–February and March–May seasons showing the greatest increases (Jones et al., 1999).

This study attempts to quantify winter warming by examining the daily temperature and precipitation changes that occurred from 1951–1999, relative to daily averages for the 1932–1950 period. These daily departures (or anomalies) are analyzed individually and together to detect unusual time-series patterns and interconnections between two or more anomalies that appear to have a physical basis. As it is generally used in this report, "winter" usually refers to the Northern Hemisphere winter, from the winter solstice to the spring equinox. When the analysis includes both the Northern and Southern hemispheres, the designations NH winter or SH winter are used.

## RAW DATA

Daily precipitation and temperature observations (maximum and minimum) for the 1932–1999 period at 74 weather stations in the United States, Europe, Asia, and Australia (Fig. 1; Table 1) are divided into a base period (1932–1950) and a test

TABLE 1

Weather Stations Used in the Analysis[a]

| No. | Name | ID | P | T | ΔT | Lat | Long |
|---|---|---|---|---|---|---|---|
| 1 | Cordova, AK | 2177 | 2461 | 3.76 | 0.587 | 60.48 | -145.27 |
| 2 | Yakutat, AK | 9941 | 3873 | 4.15 | 0.515 | 59.52 | -139.63 |
| 3 | Bartow, FL | 0478 | 1354 | 22.72 | 0.983 | 27.90 | -81.55 |
| 4 | Belle Glades, FL | 0611 | 1413 | 22.60 | 0.990 | 26.65 | -80.38 |
| 5 | Alturas, CA | 0161 | 326 | 8.10 | 0.689 | 41.48 | -120.55 |
| 6 | Davis, CA | 2294 | 456 | 15.67 | 0.342 | 38.53 | -121.77 |
| 7 | Napa, CA | 6074 | 643 | 14.85 | 0.250 | 38.22 | -122.28 |
| 8 | Childs, AZ | 1614 | 468 | 17.98 | 0.460 | 34.48 | -111.70 |
| 9 | Roosevelt, AZ | 7281 | 398 | 19.98 | 0.830 | 33.67 | -111.15 |
| 10 | Prescott, AZ | 6796 | 477 | 11.96 | 0.961 | 34.65 | -112.43 |
| 11 | Chugwater, WY | 1730 | 398 | 8.17 | 0.188 | 41.75 | -104.82 |
| 12 | Moran, WY | 6440 | 598 | 2.03 | 1.549 | 43.87 | -110.58 |
| 13 | Cheyenne, WY | 1675 | 381 | 7.67 | 1.059 | 41.16 | -104.80 |
| 14 | Baudette, MN | 0515 | 566 | 3.59 | 1.887 | 48.70 | -94.58 |
| 15 | Itaska, MN | 4106 | 675 | 3.79 | 0.067 | 47.22 | -95.18 |
| 16 | Little Falls, MN | 4793 | 659 | 5.92 | 1.900 | 46.00 | -94.35 |
| 17 | Cedar Lake, WA | 1233 | 2582 | 8.62 | 0.492 | 47.27 | -121.75 |
| 18 | Olga, WA | 6096 | 728 | 9.89 | 0.860 | 48.62 | -122.80 |
| 19 | Palmer, WA | 6295 | 2304 | 9.68 | 0.783 | 47.28 | -121.85 |
| 20 | Eldorado, KS | 2401 | 870 | 13.93 | 1.185 | 37.82 | -96.85 |
| 21 | Manhattan, KS | 4972 | 847 | 13.06 | 1.375 | 39.12 | -96.58 |
| 22 | McPherson, KS | 5152 | 755 | 13.53 | 1.170 | 38.38 | -97.65 |
| 23 | Dickinson, ND | 2188 | 415 | 4.98 | 1.437 | 46.88 | -102.62 |
| 24 | Mandan, ND | 5479 | 417 | 5.37 | 1.749 | 46.82 | -100.92 |
| 25 | Minot, ND | 5993 | 436 | 4.38 | 1.213 | 48.18 | -101.30 |
| 26 | Brenham, TX | 1048 | 1056 | 20.26 | 1.828 | 30.17 | -96.40 |
| 27 | Kaffman, TX | 4705 | 1006 | 18.30 | 0.892 | 32.57 | -96.28 |
| 28 | Lubbock, TX | 5411 | 466 | 15.75 | 1.082 | 33.67 | -101.82 |
| 29 | Farmington, ME | 2765 | 1150 | 5.86 | 0.042 | 44.68 | -70.15 |
| 30 | Lewiston, ME | 4566 | 1132 | 7.84 | 0.588 | 44.10 | -70.22 |
| 31 | Presque Isle, ME | 6937 | 937 | 4.62 | -0.162 | 46.65 | -68.00 |
| 32 | Donora, PA | 2190 | 937 | 12.08 | 0.602 | 40.17 | -79.88 |
| 33 | Erie, PA | 2682 | 1002 | 9.57 | 1.470 | 42.08 | -80.18 |
| 34 | York, PA | 9933 | 1056 | 11.92 | 0.981 | 39.92 | -76.75 |
| 35 | Linkoping, Sweden | 8525 | 514 | 6.38 | 2.366 | 68.40 | 15.53 |
| 36 | Falun, Sweden | 0537 | 587 | 4.63 | 2.925 | 60.62 | 15.62 |
| 37 | Basel, Switzerland | 1940 | 790 | 10.25 | 1.504 | 47.55 | 7.58 |

(*table continues*)

TABLE 1 (Continued)

| No. | Name | ID | P | T | ΔT | Lat | Long |
|---|---|---|---|---|---|---|---|
| 38 | Lugano, Switzerland | 9480 | 1655 | 12.39 | 1.185 | 46.00 | 8.97 |
| 39 | Zurich, Switzerland | 3700 | 1105 | 9.55 | 1.239 | 47.38 | 8.57 |
| 40 | Saentis, Switzerland | 2220 | 2440 | -0.33 | 0.695 | 47.25 | 9.35 |
| 41 | Geneva, Switzerland | 8440 | 904 | 10.26 | 1.208 | 46.25 | 6.13 |
| 42 | Uccle, Belgium | 6447 | 799 | 10.24 | 1.257 | 50.80 | 4.35 |
| 43 | Paris, France | 7150 | 626 | 11.74 | 1.470 | 48.82 | 2.33 |
| 44 | Chateauroux, France | 7354 | 720 | 11.28 | 1.343 | 46.87 | 1.72 |
| 45 | Lyon, France | 9001 | 800 | 11.63 | 1.375 | 45.72 | 4.93 |
| 46 | Bamberg, Germany | 4063 | 644 | 8.83 | 1.568 | 49.88 | 10.88 |
| 47 | Potsdam, Germany | 3342 | 582 | 9.08 | 1.736 | 52.38 | 13.07 |
| 48 | Berlin, Germany | 3319 | 586 | 8.89 | 1.788 | 52.45 | 13.30 |
| 49 | Karlsruhe, Germany | 2698 | 745 | 10.12 | 1.749 | 51.12 | 8.38 |
| 50 | Dresden, Germany | 3244 | 656 | 9.05 | 1.798 | 51.12 | 13.68 |
| 51 | Stuttgart, Germany | 2716 | 680 | 8.90 | 1.435 | 48.72 | 9.22 |
| 52 | De Bilt, Netherlands | 6260 | 802 | 9.48 | 1.566 | 52.10 | 5.18 |
| 53 | Groningen, Netherlands | 6280 | 804 | 8.84 | 1.557 | 53.13 | 6.58 |
| 54 | Maastricht, Netherlands | 6380 | 687 | 9.93 | 1.370 | 50.92 | 5.70 |
| 55 | Oxford, England | 6225 | 639 | 9.63 | 1.178 | 51.77 | -1.27 |
| 56 | Wrangel Island, Russia | 1982 | 219 | -11.09 | 0.613 | 69.97 | 178.53 |
| 57 | St. Petersburg, Russia | 6063 | 611 | 5.04 | 2.535 | 59.97 | 30.30 |
| 58 | Mokp'o, Korea | 7165 | 1112 | 14.33 | 1.353 | 34.78 | -126.38 |
| 59 | Almaty, Kazakhstan | 6870 | 625 | 9.62 | 0.958 | 43.23 | 77.93 |
| 60 | Turkestan, Kazakhstan | 8198 | 181 | 12.25 | 0.575 | 43.27 | 68.22 |
| 61 | Kiev, Ukraine | 3345 | 662 | 7.48 | -0.397 | 50.40 | 30.45 |
| 62 | Odessa, Ukraine | 3837 | 433 | 8.41 | -1.356 | 46.48 | 30.63 |
| 63 | Torrevieja, Spain | 7038 | 254 | 17.97 | 1.176 | 37.97 | 0.70 |
| 64 | San Sebastian, Spain | 8027 | 1564 | 13.13 | 1.220 | 43.30 | 2.05 |
| 65 | Darwin, Australia | 4120 | 1675 | 27.18 | 0.062 | -12.48 | -130.87 |
| 66 | Broome, Australia | 4203 | 573 | 26.62 | -0.068 | -17.95 | -122.22 |
| 67 | Port Hedlund, Australia | 4312 | 315 | 26.02 | 0.820 | -20.37 | -118.62 |
| 68 | Cape Leeuwin, Australia | 4601 | 1011 | 16.65 | -0.105 | -34.37 | -115.12 |
| 69 | Esperance, Australia | 4638 | 662 | 16.60 | 0.217 | -33.82 | -121.88 |
| 70 | Cairnes, Australia | 4287 | 1918 | 24.80 | 0.250 | -16.88 | -145.75 |
| 71 | Alice Springs, Australia | 4326 | 271 | 13.22 | 0.779 | -23.80 | -133.90 |
| 72 | Charleville, Australia | 4510 | 485 | 20.63 | 0.556 | -26.20 | -146.27 |
| 73 | Kalgoorie, Australia | 4637 | 267 | 18.33 | 0.373 | -30.77 | -121.45 |
| 74 | Mildura, Australia | 4693 | 285 | 10.07 | -0.237 | -34.22 | -142.08 |

[a]Abbreviations: ID = identification number assigned by agency that collected the data; P = mean annual precipitation, 1932–1999 period (mm); T = mean annual temperature, 1932–1999 period (°C); ΔT = NH winter temperature change (1990–1999 minus 1951–1989 means).

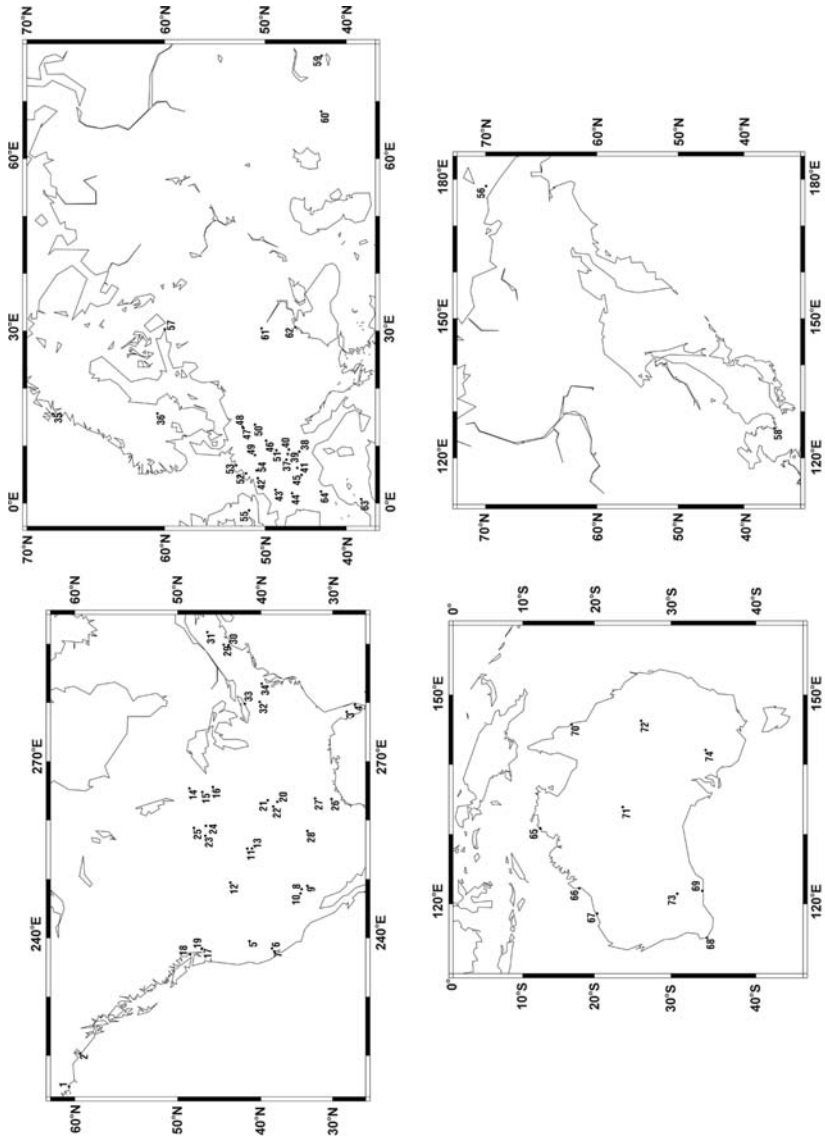


**Fig. 1.** Location of weather stations used in this report.

period (1951–1999) for analysis. The annual means for the 74 temperature and precipitation records range from –11° to 27°C, and from 181 to 3900 mm/yr, or from Arctic to subtropical to desert regimes. The years 1932–1950 are used for a base period rather than the more established 1961–1990 period, even though 1932–1950 includes part of the unusually warm period of 1925–1944. For an unbiased analysis, it is felt that the test period should be independent and chronologically later than the base period, especially when daily observations are used. Station homogeneity is addressed whenever possible by selecting weather stations with a minimum of missing observations, those that have not been frequently moved, and are not in large cities. There are several obvious exceptions to the large-city criterion, but a majority of the 74 stations are located in rural areas or small towns.

## ANALYSIS

Five daily departure variables are determined for the 1951-99 test period: (1) maximum daily temperature ($t_x$); (2) minimum daily temperature ($t_n$); (3) mean daily temperature $(t_x + t_n)/2$; (4) mean daily temperature range $(t_x - t_n)$; and (5) mean daily precipitation (p). Each of these variables is calculated for each of the 74 weather records for the 49-year test period by the following procedures. First, the daily mean temperature and temperature range on day (i), year (n), and weather station (k) are calculated from the measured maximum and minimum daily temperatures:

$$t_d(i, n,k ) = (t_x(i, n, k) + t_n(i, n, k))/2,$$

$$d_{tr}(i, n, k) = (t_x(i, n, k) – t_n(i, n, k)).$$

The average temperature for each day (i) of the base period (1932–1950) for each station (k) is determined as:

$$t_a(i, k) = \sum_{n = 1932}^{n = 1950} (t_d(i, n, k))/19 .$$

The temperature anomaly for each day of the test period (1951–1999) is then

$$\Delta t(i, n, k) = t_d(i, n, k) – t_a(i, k).$$

Similarly, the average temperature range for each day of the base period is calculated for each station as:

$$d_{tra}(i, k) = \sum_{n = 1932}^{n = 1950} (d_{tr}(i, n, k))/19 ,$$

from which the temperature range anomaly for each day of the test period is calculated:

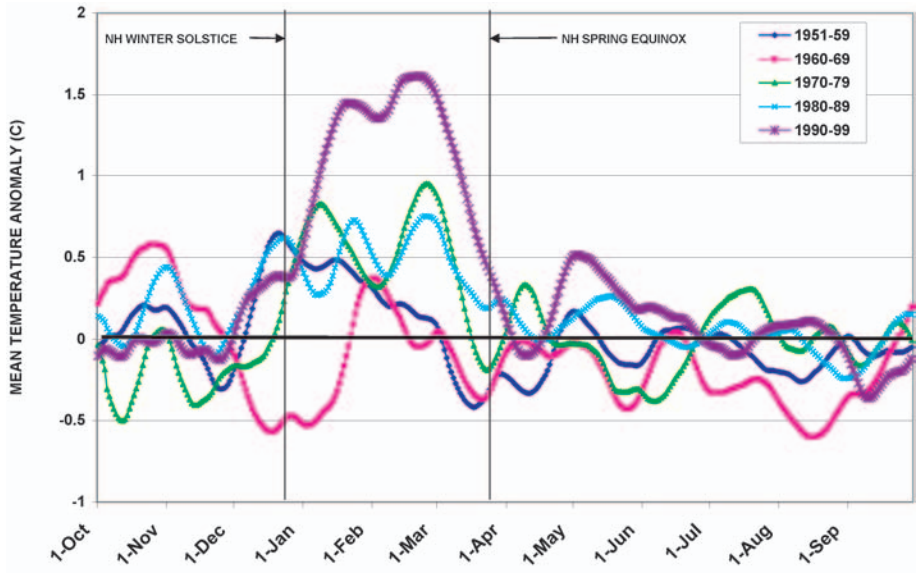


**Fig. 2.** Decadal changes in mean temperature anomalies from 1951 to 1999, average of 74 stations in Northern and Southern hemispheres.

$$\Delta t_{tr}(i, n, k) = d_{tr}(i, n, k) - d_{tra}(i, k).$$

The same procedure is carried out for daily precipitation and maximum and minimum temperature observations to obtain the daily precipitation anomaly from the 1932–50 average, $\Delta p_p(i,n,k)$; the daily maximum temperature departure, $\Delta t_{tx}(i, n, k)$, and daily minimum temperature departure, $\Delta t_{tn}(i, n, k)$.

To account for differences in the time of observations and other data collection discrepancies, $\Delta t(i, n, k)$, $\Delta t_{tr}(i, n, k)$, $\Delta p_p(i, n, k)$, $\Delta t_{tx}(i, n, k)$, and $\Delta t_{tn}(i, n, k)$ are smoothed by a 21-day running average plotted at mid-point—i.e., each day is an average of 10 days prior to and 10 days following—plus the temperature, temperature range, or precipitation on the day under consideration.

The average annual precipitation and temperature is shown for each weather station listed in Table 1, plus the winter temperature change that occurred for the 1990–1999 period relative to 1951–1989. Of the 74 stations in the study, 6 show negative departures during the last decade in this analysis.

## WINTER WARMING

There is a distinct seasonal pattern in mean temperature anomalies that began in the mid-1980s and has become more prominent nearly every year since then. Figure 2 gives examples of temperature anomalies averaged for decadal time spans during the 1951–1999 test period. The 1990–1999 average demonstrates the strongest winter-warming signal compared to the previous four decades. The peak positive temperature departure averaged for the 1990–1999 period is approximately 1.5°C, on March 1. A similar pattern is repeated each year within the 1990–1999 period, except

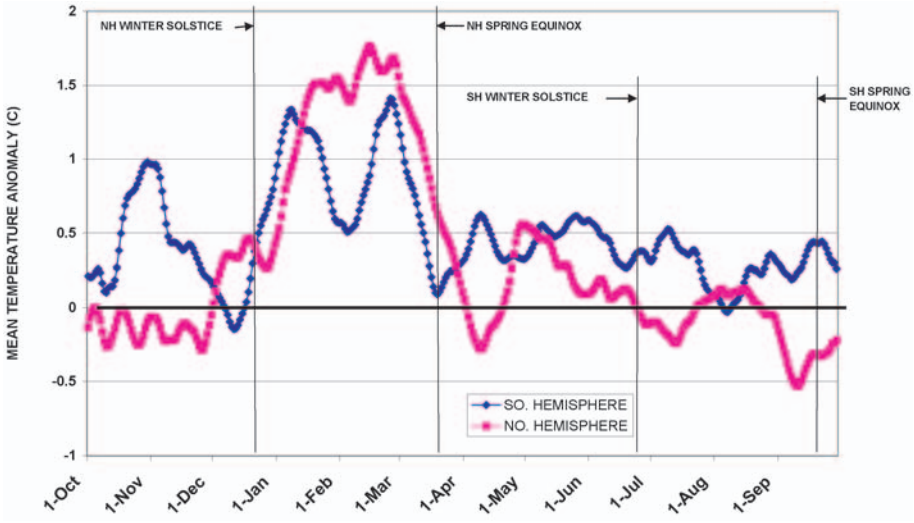


**Fig. 3.** Mean temperature anomalies (1990–1999 average) for 64 Northern Hemisphere and 10 Southern Hemisphere stations.

in 1995–1996, when both temperature and precipitation anomalies were negative. The 1995–1996 minimum may be related to cooler SST in the Eastern Pacific that year (a La Niña event). The diurnal temperature range anomalies were only slightly positive during the 1995–1996 winter and the minimum temperature and precipitation anomalies were negative, signifying below-normal atmospheric water vapor. Although the strongest warming signal in the last decade occurs between the Northern Hemisphere winter solstice and the spring equinox, a link to sun angle is likely not significant.

Although the signal is weaker and bimodal, the Southern Hemisphere temperature anomalies also indicate warming during the Northern Hemisphere winter, but unexpectedly, insignificant warming during the Southern Hemisphere winter (Fig. 3). The bimodal pattern of global winter precipitation anomalies shown in Figure 4 appears to have a slight link to winter temperature anomalies; however, there is a much stronger pattern similarity between Northern Hemisphere precipitation and Southern Hemisphere temperature (Fig. 5).

The bimodal pattern that occurs between the Northern Hemisphere winter solstice and spring equinox for both Northern Hemisphere precipitation and Southern Hemisphere temperature, shown in greater detail in Figure 6, suggests a mutual dependency. Earlier studies have found evidence of a positive feedback between temperature and atmospheric water vapor, which more than doubles the warming relative to fixed water vapor (Hall and Manabe, 1999). Atmospheric water vapor is an effective greenhouse gas (three times as potent as carbon dioxide); thus a self-perpetuating cycle of increasing temperatures and precipitation may now be under way on a global scale. Winter temperatures and precipitation (average of 74 stations for 90 days) have increased at approximately the same rate since 1951, and are highly correlated since 1995 (Fig. 7).

A link between Southern Hemisphere temperature and Northern Hemisphere precipitation has not been suggested previously and may be disputed as being too tenuous. Only 10 weather stations in Australia are used to represent the Southern

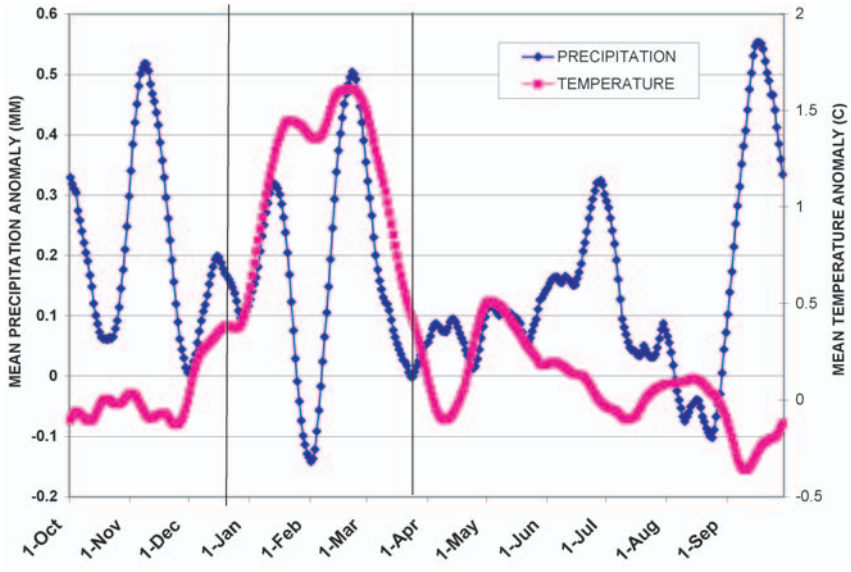


**Fig. 4.** Temperature and precipitation anomalies averaged for the 1990–1999 period and for 74 global stations.

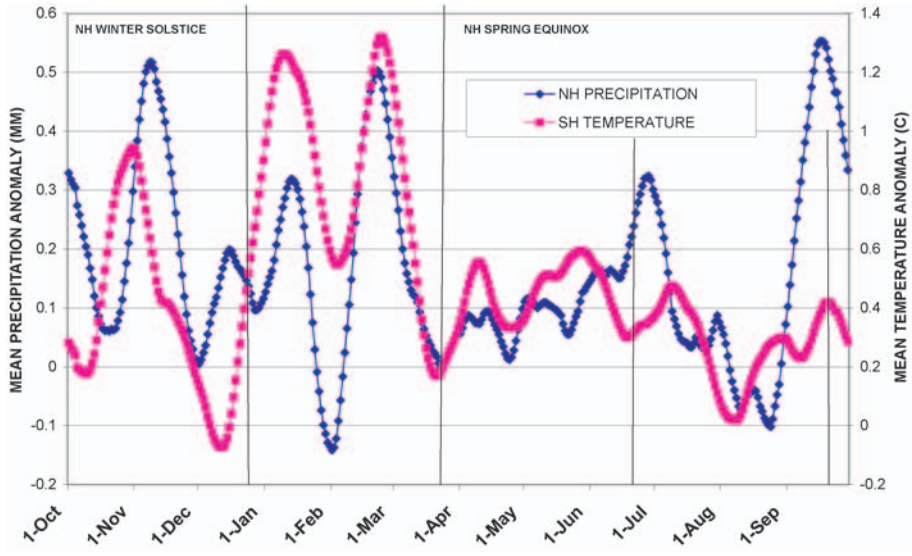


**Fig. 5.** Northern Hemisphere precipitation anomalies (averge of 64 stations) and Southern Hemisphere temperature anomalies (average ov 10 stations), both averaged for the 1990–1999 period.

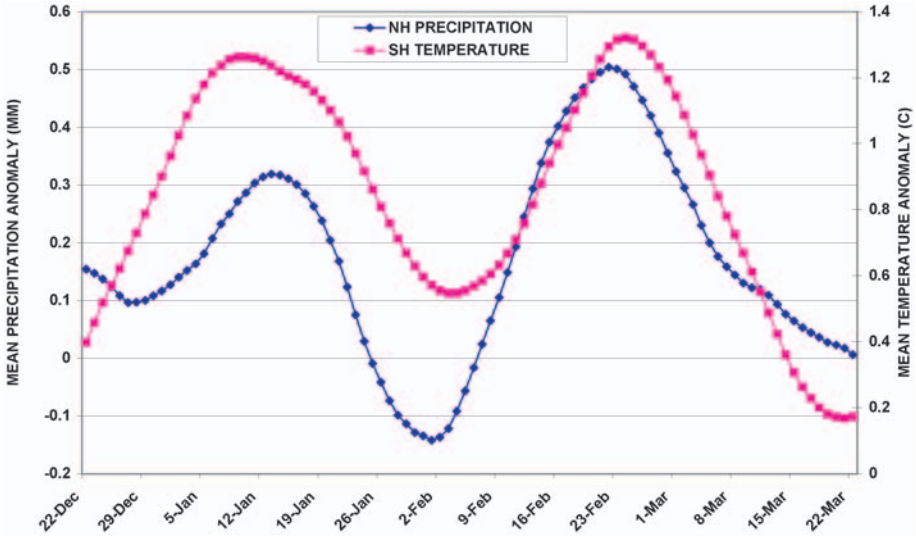


**Fig. 6.** Northern Hemisphere precipitation anomalies (average of 64 stations) and Southern Hemisphere temperature anomalies (average of 10 stations), both averaged for the 1990–1999 period (enlargement of Figure 4).

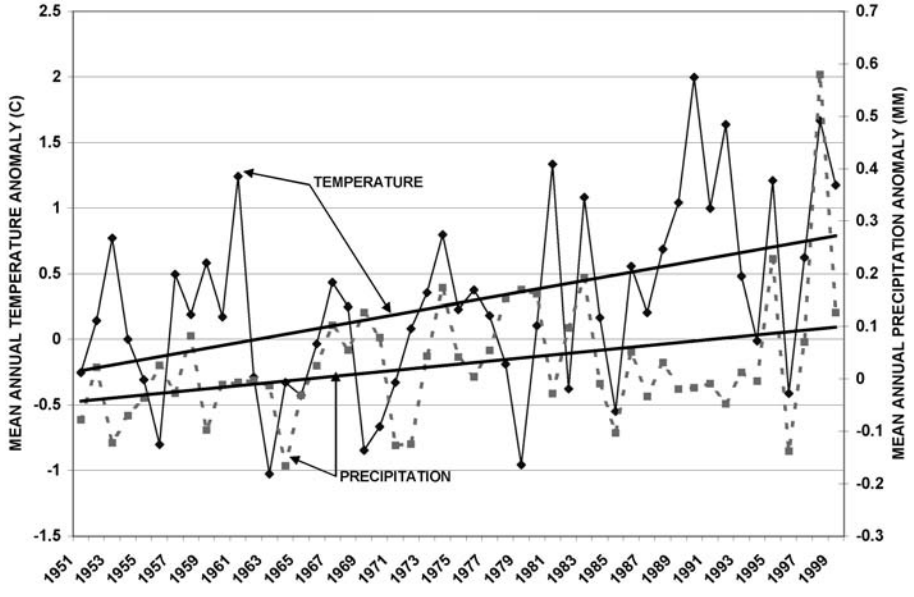


**Fig. 7.** Temperature and precipitation anomaly trends, averaged for the January–March season and for 74 global stations.

Hemisphere; however, all of these stations have a similar NH winter pattern to that shown in Figure 3. It is the industrialized countries in the Northern Hemisphere that have produced a major proportion of the Earth's greenhouse gases (estimated at 95%). Rapid diffusion of $CO_2$ and other anthropogenic gases occurs from the Northern to the Southern Hemisphere so it is more likely that Southern Hemisphere warming is being forced by Northern Hemisphere atmospheric conditions, rather than vice versa. If the current climate change is caused by an unprecedented increase in atmospheric concentrations of carbon dioxide, it would be expected that the atmosphere over the entire Earth would be affected. Therefore, it is logical to conclude the winter warming signal observed equally in both hemispheres is linked to recent changes in the NH atmosphere due to human activities. The observed increase shown for Southern Hemisphere temperatures *during the Northern Hemisphere winter* could then be considered a clear signal of global warming caused by anthropogenic greenhouse gases.

Another positive feedback mechanism may be under way that is driven mainly by NH conditions. As the altitude of the snowline rises due to higher wintertime temperatures, the surface area of the earth covered by snow decreases, reducing its reflectivity (Groisman et al., 1994). The resulting lower albedo over the land areas of the earth will cause more solar radiation to be absorbed, thus raising temperatures even more. The reason why warming occurs during the NH winter rather than the summer season may then be due to the positive feedback effect of a reduced NH winter snow-cover extent.

## SYNCHRONIZED TEMPERATURE ANOMALIES

Each of the 74 stations, located between 70° N and 34° S Latitude, and 146° W and 178° E Longitude, begin to show similar seasonal patterns in the 1980s, when for a few days each year over 95 percent of the stations are synchronized (have positive temperature anomalies on the same day). This phenomenon always occurs during the winter season. The fraction of synchronized stations tends to not exceed ~0.50–0.60 until the 1980s, when fractions greater than 0.90 begin to occur. The first time the fraction reached 0.946 (70 stations had temperatures above normal on the same day) is January 13, 1990, which was then followed by approximately 100 days in which the share exceeded 0.90 throughout the 1990s. Figure 8 shows the fraction of the 74 weather stations that have positive anomalies on the same day, together with the average daily temperature anomaly (both averaged for the 1990–1999 period).

There is an inexplicable connection between the number of synchronized stations with temperature anomalies and the mean temperature anomaly. It is proposed that the similarity in patterns occurs because both are the result of climate-forcing by an external mechanism, not directly related to global circulation in the atmosphere. For example, if solar radiation intensity had been steadily increasing during the NH winter months over the past 20 years, temperatures over most of the Earth would have risen evenly and simultaneously, and the results shown in Figure 8 could be readily explained. However, no evidence exists that wintertime solar intensity has increased by the amount needed to produce positive temperature anomalies of this magnitude. Solar variability may play a significant role in regional surface temperatures but on a global scale its influence is insignificant (Shindell et al., 1999). Therefore, another

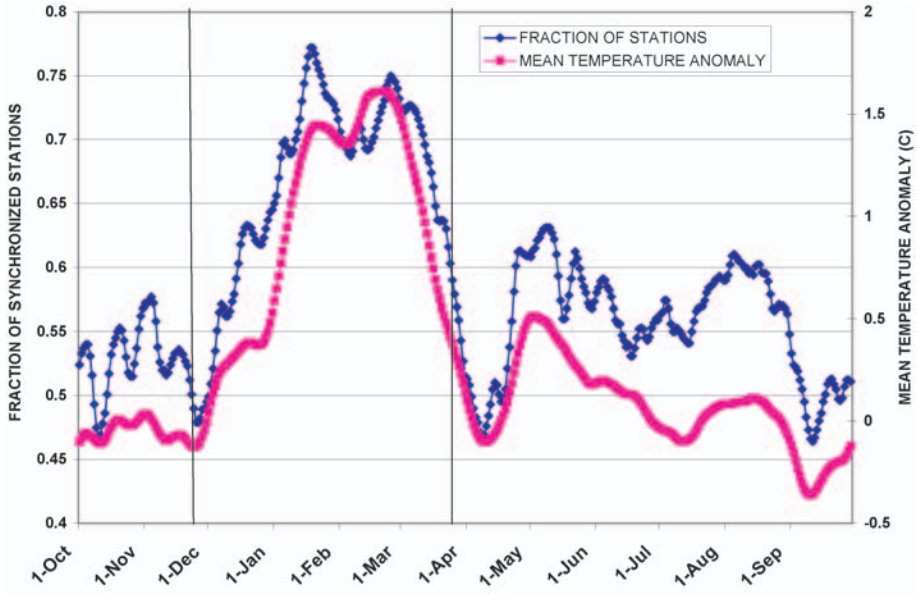


**Fig. 8.** Mean temperature anomalies (average of 74 stations) and fraction of these 74 stations that show positive temperature departures on the same day (both averaged for the 1990–1999 period).

climatic anomaly must be present to produce these results. One possibility is an efficiently operating positive feedback system fueled by increasing concentrations of atmospheric greenhouse gases (currently rising at 0.4 % per year) and increasing amounts of atmospheric water vapor. These conditions would tend to affect surface temperatures over most of the Earth, evenly and simultaneously. It would also explain the apparent high correlation between the fraction of synchronized temperature stations and positive temperature anomalies shown in Figure 8. Although a direct cause and effect mechanism relating the 15% increase in greenhouse gases since 1958 to these temperature changes has not been found, empirical evidence for its influence is substantial (Karl and Trenberth, 2003).

A global mechanism has been proposed that could synchronize the timing and magnitudes of warming and cooling in the Northern and Southern hemispheres (Lynch-Stieglitz, 2004). Although a much longer time scale is considered (hundreds or thousands of years versus days or months), synchronized hemispheric climates would require a change in the greenhouse capacity of the atmosphere or in the amount of sunlight absorbed by the Earth, both of which are mentioned as possible causes of the recently observed synchronized temperature phenomenon noted above.

## LINKING THE DIURNAL TEMPERATURE RANGE AND PRECIPITATION WITH TEMPERATURE

The daily range between the maximum and minimum temperature has been used as a proxy for cloudiness in other studies (Karl et al., 1984; Tangborn et al., 1991; Dai

et al., 1997a). From a practical standpoint the diurnal temperature range is a useful tool, because long term and consistent cloud cover observations are scarce or are nonexistent in many regions. However, there are causes other than cloudiness for variations in the temperature range, such as changes in atmospheric water vapor, which are related to the daily minimum (nighttime) temperature. During the past five decades, the average global daily minimum temperature (as measured at the 74 weather stations) increased 1.8°C (0.36°C per decade), while the maximum increased 1.3°C (0.26°C per decade); thus the average temperature range has declined. The rate of increase in minimum temperature is two times greater than that reported in an earlier study (Karl et al., 1993b), which may be partly due to the difference in observation periods. One reason for the increase in minimum temperatures is reasoned to be due to rising concentrations of atmospheric water vapor, which is an efficient greenhouse gas that traps solar radiation and raises nighttime temperatures. Sixty percent of the Earth's greenhouse effect with clear skies is due to water vapor (IPCC, 2001).

Clouds are intimately connected to the water vapor pattern, and observed precipitation is a measure of the concentration of water vapor in the atmosphere. Water vapor feedback is considered to be the most important feedback effect and produces the greatest warming in general circulation models (IPCC, 2001). Therefore, segregating temperature anomalies based on the temperature range and precipitation anomalies may lead to an improved understanding of the water vapor/temperature feedback system. Other studies have confirmed the presence of a positive feedback mechanism between increasing temperatures and water vapor (Rind et al., 1991).

Temperature-range anomalies are applied to simulate a water vapor variable and used to segregate minimum temperature anomalies into days with above-normal water vapor and days that are below normal. Minimum temperature is used rather than the mean, because it is more closely associated with atmospheric water vapor.

For each weather station (k) two data files are considered simultaneously, namely the daily temperature range anomalies for the 1951–1999 period, and minimum temperature anomalies for the same period, and each day (i) of the 1951–1999 period is segregated according to the precipitation or temperature range departure for that day. For example, starting on October 1, 1951, if the daily temperature range anomaly is negative, the mimimum temperature anomaly for that day is placed in the negative bin. If it is positive, it is stored in the positive bin. The values in both bins are summed through the water year and the number of positive or negative temperature range anomalies noted on September 30, at the end of the water year. Thus:

$$\Delta t_{pos}(n, k) = \sum_{i=1}^{365} \Delta t(i, n, k) \quad \text{if } \Delta t(i, n, k) > 0 ,$$

$$\Delta t_{neg}(n, k) = \sum_{i=1}^{365} \Delta t(i, n, k) \quad \text{if } \Delta t((i, n, k) < 0 .$$

The average minimum temperature in each category is obtained by dividing by the number of days with a positive ($n_{dpos}$) or negative ($n_{dneg}$) temperature range anomaly:

$$\Delta t_{pos}(n, k) = \Delta t_{pos}(n, k)/n_{dpos},$$

$$\Delta t_{neg}(n, k) = \Delta t_{neg}(n, k)/n_{dneg}.$$

After calculating these annual values for all stations, an average annual value for each category based on the 74 stations is calculated:

$$\Delta t_{pos}(n) = \sum_{k=1}^{74} \Delta t_{pos}(n, k)/74,$$

$$\Delta t_{neg}(n) = \sum_{k=1}^{74} \Delta t_{neg}(n, k)/74.$$

Finally cumulative values are calculated for the years m = 1951–1999:

$$sm_{pos}(m) = \sum_{n=1951}^{m} \Delta t_{pos}(n),$$

$$sm_{neg}(m) = \sum_{n=1951}^{m} \Delta t_{neg}(n).$$

Since 1985, the mean minimum temperature anomaly has been predominantly positive on days with both high and low temperature ranges (ostensibly both clear and cloudy days). A plot of cumulative minimum temperature anomalies ($sm_{pos}(n)$ and $sm_{neg}(n)$) based on the temperature range for the 1951–1999 period is shown in Figure 9. The cumulative values of $\Delta t_{pos}(n)$ and $\Delta t_{neg}(n)$ are plotted rather than individual years so that each year will reflect temperature anomalies in previous years. The temperature range departure as it is used here likely does not simulate actual cloud cover conditions on most of the 17,520 days used in this analysis, as much as it depicts atmospheric water vapor, which will also determine maximum and minimum temperature departures, and thus the temperature range. After approximately 1985, there is an intriguing similarity in the trends shown in Figure 9. Both are generated by positive and negative values of the daily temperature range anomalies, and suggest a positive feedback between the daily mean temperature and the temperature range, which is linked to cloudiness and water vapor.

Segregation of daily temperature anomalies using daily precipitation anomalies produces results similar to those found using the temperature range (Fig. 10). The steady decline in temperature anomalies until about 1980 when precipitation is below normal, and its abrupt change in direction after 1980, suggests a major change in atmospheric stability occurred then. It is noteworthy that since the mid-1980s the temperature is rising at the same rate during both wet and dry conditions. The trends

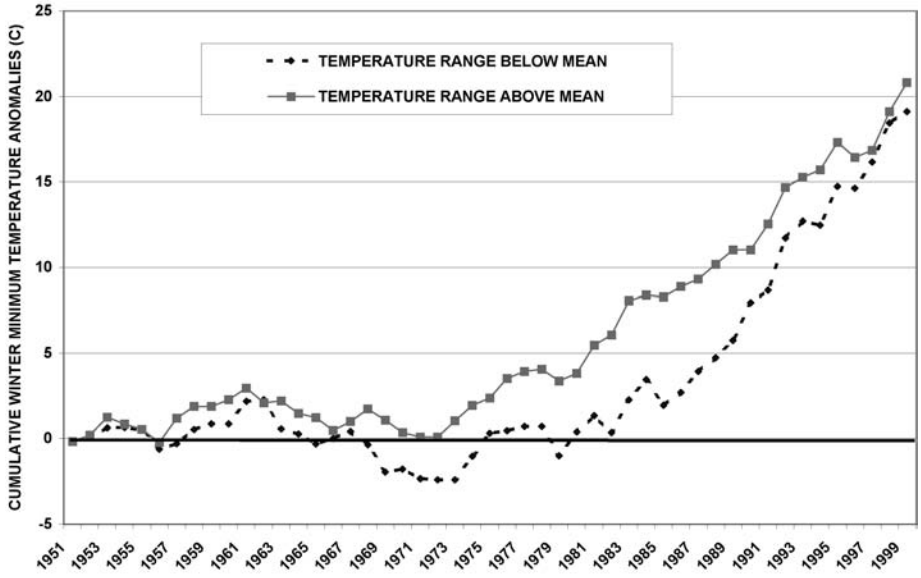


**Fig. 9.** Segregation of daily minimum temperature anomalies based on the daily temperature range anomalies (daily maximum minus minimum), cumulated annually from 1951–1999 (74 station averages).

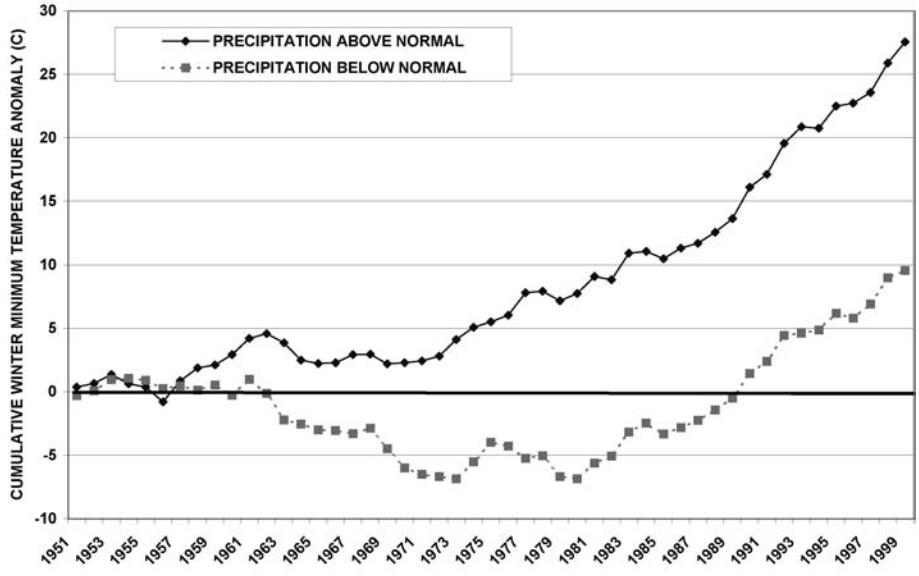


**Fig. 10.** Segregation of daily minimum temperature anomalies based on the daily precipitation anomalies, cumulated annually from 1951 to 1999 (74-station averages).

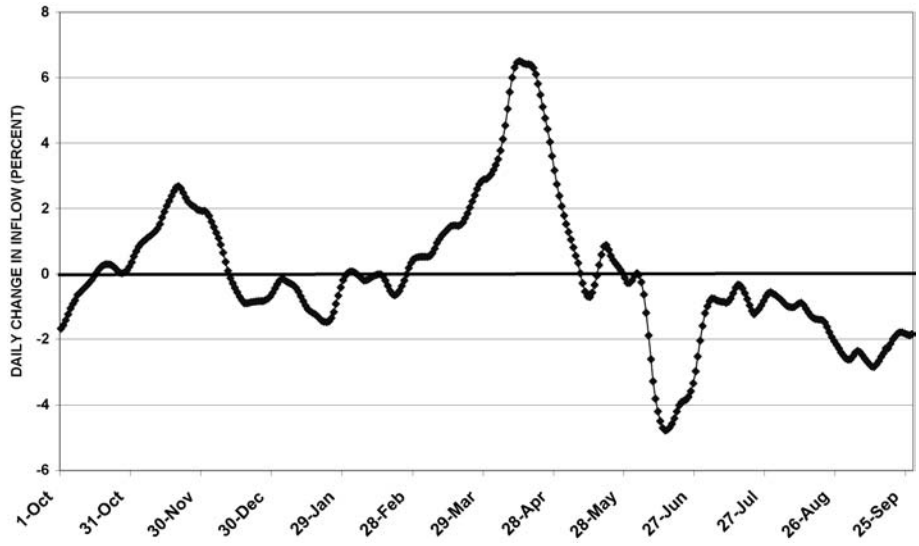


**Fig. 11.** Change in daily natural inflows of Columbia River at Grand Coulee Dam (1986–2002 mean minus 1969–1985 mean).

shown in Figures 9 and 10 could be considered a quasi–heat index of an atmosphere that has been steadily warming since about 1985.

## CONSEQUENCES OF WARMER WINTERS

Based on the mean global lapse rate of 0.65°C/100 m, a mean temperature increase of 1.5°C will raise the freezing level approximately 230 meters (750 feet). A higher wintertime freezing level in mountainous regions translates to less snowfall and more rain, which means increased runoff in the winter and spring and less during the summer months. In some regions, spring and autumn flooding will be more severe due to increased snowmelt augmented by precipitation as rain rather than snow. A change in the seasonal pattern of streamflow derived from snowmelt will affect hydroelectric generation, water diverted for irrigation, and salinity variations of estuaries and offshore ocean currents. Therefore, three major industries (energy, agriculture, and fisheries) will need revised management plans in future years if these climate changes continue at the present rate.

An example of the change in runoff patterns induced by warmer winters is depicted in Figure 11, which shows the change in daily inflow that has occurred for the Columbia River at Grand Coulee Dam in Washington state. There has been as much as an average 6% increase in spring runoff during the 17-year period 1986–2002 compared to the previous 17-year average. At the same time summer and autumn (June–September) runoff has declined as much as 5%. The springtime increase is likely due to increased snowmelt at higher altitudes and an increase in precipitation as rain. The summer decline is caused by a deficient high-altitude snowpack. A loss in the volume of the mountain snowpack is detrimental for optimum hydroelectric energy generation because it reduces the flexibility of managing large

reservoirs, which may not be able to accommodate the increase in winter runoff. In addition to affecting energy production, alteration of the seasonal distribution of streamflow will impact agriculture by decreasing water supplies for irrigation during the summer months. Recent changes in precipitation patterns in the Great Plains have been attributed to changes in surface water temperatures in the Pacific Ocean and corresponding atmospheric conditions (Rossel and Garbrecht, 2000).

The mass balance of glaciers will also be affected by higher freezing levels and less snow at altitudes that have a large proportion of a glacier's total area. A deficient winter snowpack would allow low-albedo ice to become exposed earlier in the season, increasing ablation rates by an order of magnitude. Mass balances of glaciers in Alaska may already have become predominantly negative (Arendt et al., 2002; Muskett et al., 2003). Many of the large Alaskan glaciers have a significant proportion of their area that is nearly flat, so that a 250-meter rise in the snowline will decrease the balance of many hundred square kilometers of glacier area. Models of continental-scale ice sheets demonstrate the extreme sensitivity of large glaciers to minute seasonal temperature changes (Roe and Lindzen, 2001). Increased ablation rates of present-day ice sheets in Antarctica and Greenland with a subsequent rise in sea level is another probable consequence of higher temperatures. An increase in freshwater runoff from rapidly melting glaciers in Alaska is believed to have altered offshore Pacific Ocean currents and affected salmon migration (Tangborn et al., 2000). The multi-billion dollar ski industry will of course also be adversely affected by a several hundred meter rise in the freezing level and snowline.

## CONCLUSIONS

Winter (January–March) temperature anomalies at 74 weather stations have been increasing at a higher rate than annual temperatures. One apparent reason for this difference is that summer and autumn (April–December) temperature anomalies have been stable or decreasing. At most weather stations used in this study, there are striking patterns of a December low and a January or February high since about 1990. A possibly significant finding is that temperatures in the Southern Hemisphere are also increasing *during the Northern Hemisphere winter.* However, additional testing is needed to confirm this result, which if true would be an unprecedented finding. Long-term (1932–2002) historical records of daily temperature and precipitation observations from Southern Hemisphere stations are required, but seem to be non-existent (or extremely scarce), except for the 10 records from Australia used in this study.

Winter temperatures among the 74 stations are becoming more synchronized (demonstrating positive departures on approximately the same day) since about 1990. Therefore the cause of the recently observed winter warming is likely a global phenomenon not related to general atmospheric circulation.

Associated with winter warming is an increase in positive precipitation anomalies and in negative diurnal temperature range anomalies, indicating increased precipitation and atmospheric water vapor during the warmer winters and introducing the possibility of an established positive temperature/precipitation feedback mechanism. More research is needed to determine if the effect is irreversible. The higher correlation between minimum temperature and precipitation anomalies for the past decade is

the apparent result of increasingly higher concentrations of water vapor causing a rise in nighttime temperatures.

Analysis of winter temperature anomalies as segregated by historical changes in temperature range and precipitation anomalies reveals an abrupt climate shift in the mid-1980s. These changes suggest a steady warming of the earth's atmosphere since 1985.

## LITERATURE

**Arendt, A., K. A. Echelmeyer, W. D. Harrison, C. S. Lingle, and V. B. Valentine.** "Rapid wastage of Alaska glaciers and their contribution to rising sea level," *Science*, Vol. 297, 2002, pp. 382-389.

**Dai, A., A. D. Del Genio, and I. Y. Fung.** "Clouds, precipitation, and temperature range," *Nature*, Vol. 386, 1997a, pp. 665-666.

**Dai, A., I. Y. Fung, and A. D. Del Genio.** "Surface observed global land precipitation variations during 1900-1988," *Journal of Climate*, Vol. 10, 1997b, pp. 2943-2962.

**Groisman, P. Ya., T. R. Karl, R. W. Knight, and G. L. Stenchikov.** "Changes in Snowcover, Temperature, and Radiation Heat Balance over the Northern Hemisphere," *Journal of Climate*, Vol. 7, 1994, pp. 1633-1656.

**Hall, A. and S. Manabe.** "The role of water vapor feedback in unperturbed climate variability and global warming," *Journal of Climate*, Vol. 12, 1999, pp. 2327-2346.

**IPCC (International Panel of Climate Change).** *Climate Change 2001: The Scientific Basis. Contribution of Working Group I to the Third Assessment Report of the Intergovernmental Panel on Climate Change* (J. T. Houghton, Y. Ding, D. J. Griggs, M. Noguer, P. J. van der Linden, X. Dai, K. Maskell, and C. A. Johnson, eds.). Cambridge University Press, 2001, 881 pp.

**Karl, T. R., P. D. Jones, R. W. Knight, G. Kukla, N. Plummer, V. Razuvayev, K. P. Gallo, J. Lindsey, R. J. Charlson, and T. C. Peterson.** "A new perspective on recent global warming—Asymmetric trends of daily maximum and minimum temperatures," *Bulletin of the American Meteorological Society*, 1993, pp. 1007-1023.

**Karl, T. R., G. Kukla, and J. Gavin.** "Decreasing diurnal temperature range in the United States and Canada, 1941–1980," *Journal of Climatology and Applied Meteorology*, Vol. 23, 1984, pp. 1489-1504.

**Karl, T. R. and K. E. Trenberth.** "Modern global climate change," *Science*, Vol. 302, December 5, 2003, pp. 1719-1723.

**Jones, P. D., M. New, D. E. Parker, S. Martin, and I. G. Rigor.** "Surface air temperature and its changes over the past 150 years," *Reviews of Geophysics*, Vol. 37, May 2, 1999, pp. 173-199.

**Lindzen, R. S., M. D. Chou, and A. Hou.** "Does the Earth have an adaptive infrared iris?" *Bulletin of the American Meteorological Society*, Vol. 82, No. 3, 2001, pp. 417-432.

**Lynch-Stieglitz, J.** "Hemisphere asynchrony of abrupt climate change," *Science*, Vol. 304, 2004, pp. 1919-1920.

**Muskett, R. R., C. S. Lingle, W. V. Tangborn, and B. T. Rabus.** "Multi-decadal elevation changes on Bagley Ice Valley and Malaspina Glacier, Alaska," *Geophysical Research Letters*, Vol. 30, No. 16, 2003, pp. 1-1 to 1-4.

**Otterman, J., J. K. Angell, J. Ardizzone, R. Atlas, S. Schubert, and D. Starr.** "North Atlantic surface winds as a source of winter warming in Europe," *Geophysical Research Letters*,Vol. 29, No. 19, 2002, pp. 18-1 to 18-4.

**Rind, D., E. W. Chiou, W. Chu, J. Larsen, S. Oltmans, J. Lerner, M. P. McCormick, and L. McMaster.** "Positive water vapour feedback confirmed in by satellite data," *Nature*, Vol. 349, 1991, pp. 500-503.

**Rind, D., D. Shindell, P. Lonergan, and N. K. Balachandran.** "Climate change and the middle atmosphere, part III: The doubled $CO_2$ climate revisited," *Journal of Climate*, Vol. II, 1998, pp. 876-894.

**Roe, G. H. and R. S. Lindzen.** "The mutual interaction between continental-scale ice sheets and Atmospheric Stationary Waves," *Journal of Climate*, Vol. 14, 2001, pp. 1450-1465.

**Rossel, F. E. and J. D. Garbrecht.** "Pacific sea surface temperature and precipitation in the Southern Great Plains," in: *Proceedings of the 12th Conference on Applied Climatology, Asheville, North Carolina, 8–10 May 2000*. American Meteorological Society, paper 10A.6, p. 233-236.

**Russell, G., J. R. Miller, D. Rind, R. A. Ruedy, G. Schimdt, and S. Sheth.** "Comparison of model and observed regional temperature changes during the past 40 years," *Journal of Geophysical Research*, Vol. 105, 2000, pp. 14,891-14,898.

**Shindell, D., D. Rind, N. Balachandran, J. Lean, and P. Lonergan.** "Solar cycle variability, ozone, and climate," *Science*, Vol. 284, April 9, 1999, pp. 305-308.

**Shindell, D. T., G. A. Schmidt, R. L. Miller, and D. Rind.** "Northern Hemisphere winter climate response to greenhouse gas, volcanic, ozone, and solar forcing," *Journal of Geophysical Research*, Vol. 106, 2001, pp. 7193-7210.

**Tangborn, W., C. Ebbesmeyer, and E. R. LaChapelle.** "Hidden signals in the Washington state climate record." Paper presented at the Puget Sound Research Conference, January 4–5, 1991, Seattle, Washington.

**Tangborn, W., C. Lingle, K. Echelmeyer, and T. Royer.** "Do negative glacier balances affect the Alaska coastal current?" Abstract, Arctic Science 2000, American Association for the Advancement of Science and the Yukon Science Institute, September 21–24, 2000, Whitehorse, Yukon Territory, Canada.

**Volodin, E. M. and V. Y. Galin.** "Interpretation of winter warming on Northern Hemisphere continents in 1977–1994," *Journal of Climate*, Vol. 12, October 1999, pp. 2947-2955.

**Wallace, J. M., Y. Zhang, and L. Bajuk.** "Interpretation of the interdecadal trends in the Northern Hemisphere surface air temperatures," *Journal of Climate*, Vol. 9, 1996, pp. 249-259.

**Wetherald, R.T. and S. Manabe.** "Cloud cover and climate sensitivity," *Science*, Vol. 37, 1980, pp. 1585-1519.

**Zhang, Y., J. M. Wallace, and D. S. Battisti.** "ENSO-like interdecadal variability, 1900–1993," *Journal of Climate*, Vol. 10, 1997, pp. 1004-1020.